

# *Characteristics and Numerical Simulations of Extremely Large Atmospheric Boundary- layer Heights over an Arid Region in North-west China*

**Minjin Ma, Zhaoxia Pu, Shigong Wang  
& Qiang Zhang**

## **Boundary-Layer Meteorology**

An International Journal of Physical,  
Chemical and Biological Processes in  
the Atmospheric Boundary Layer

ISSN 0006-8314

Volume 140

Number 1

Boundary-Layer Meteorol (2011)

140:163-176

DOI 10.1007/s10546-011-9608-2

## **BOUNDARY-LAYER METEOROLOGY**

VOLUME 144 No. 1 July 2012

*An International Journal of Physical, Chemical and  
Biological Processes in the Atmospheric Boundary Layer*

*Editor: J.R. Garratt*



 Springer

ISSN 0006-8314

 Springer

**Your article is protected by copyright and all rights are held exclusively by Springer Science+Business Media B.V.. This e-offprint is for personal use only and shall not be self-archived in electronic repositories. If you wish to self-archive your work, please use the accepted author's version for posting to your own website or your institution's repository. You may further deposit the accepted author's version on a funder's repository at a funder's request, provided it is not made publicly available until 12 months after publication.**

## Characteristics and Numerical Simulations of Extremely Large Atmospheric Boundary-layer Heights over an Arid Region in North-west China

Minjin Ma · Zhaoxia Pu · Shigong Wang ·  
Qiang Zhang

Received: 24 January 2010 / Accepted: 15 March 2011 / Published online: 3 April 2011  
© Springer Science+Business Media B.V. 2011

**Abstract** Over arid regions in north-west China, the atmospheric boundary layer can be extremely high during daytime in late spring and summer. For instance, the depth of the observed convective boundary layer can exceed 3,000 m or even be up to 4,000 m at some stations. In order to characterize the atmospheric boundary-layer (ABL) conditions and to understand the mechanisms that produce such an extreme boundary-layer height, an advanced research version of the community weather research and forecasting numerical model (WRF) is employed to simulate observed extreme boundary-layer heights in May 2000. The ability of the WRF model in simulating the atmospheric boundary layer over arid areas is evaluated. Several key parameters that contribute to the extremely deep boundary layer are identified through sensitivity experiments, and it is found that the WRF model is able to capture characteristics of the observed deep atmospheric boundary layer. Results demonstrate the influence of soil moisture and surface albedo on the simulation of the extremely deep boundary layer. In addition, the choice of land-surface model and forecast lead times also plays a role in the accurate numerical simulation of the ABL height.

**Keywords** Arid region · Atmospheric boundary-layer height · Numerical simulation · Weather research and forecasting (WRF) model

---

M. Ma · S. Wang  
College of Atmospheric Sciences, Lanzhou University, Lanzhou, Gansu, China

M. Ma · Z. Pu (✉)  
Department of Atmospheric Sciences, University of Utah, 135 South 1460 East, Rm. 819, Salt Lake City,  
UT 84112, USA  
e-mail: Zhaoxia.Pu@utah.edu

Q. Zhang  
Key Laboratory of Arid Climate Change and Disaster Reduction, Institute of Arid Meteorology,  
Lanzhou, Gansu, China

## 1 Introduction

The atmospheric boundary-layer (ABL) height is a key parameter in the parametrization of atmospheric turbulent diffusion, especially in air pollution models (O'Brien 1970; Gryning et al. 1987; Davies et al. 2007). A few previous studies have shown that ABL heights have an influence on the concentration of a chemical substance (Garratt and Pearman 1973; Culf 1993; Culf et al. 1997). Oncley et al. (2004) found a strong inverse relationship between ABL heights and observed pollutant levels, and claimed that a deep ABL implies the strong mixing in the vertical direction and thus substance and energy can be transferred to high altitudes. Since the air mixture changes the energy distribution and affects atmospheric circulations that are associated with weather and climate, it is important to study the characteristics of boundary-layer heights, especially the unusually deep ABL.

Previous studies and observations have pointed out the ABL heights can be as much as 5 km in *lower* latitudes such as in India under special climatic conditions (Raman et al. 1990; Garratt 1992). Normally, the ABL height is less than 2–3 km in the middle latitudes but varies in different regions. For instance, in Europe the height of the mixed layer in the late afternoon is typically 1–2 km above the ground. However, in the middle latitudes of India, the ABL height can exceed 2 km and even 3 km or higher during summer seasons (Kumar et al. 2010). Over the Dunhuang, an arid region in north-west China, the ABL is more than 3 km high and can even reach 4 km during late spring to summer. This ABL is remarkably greater than the ABL height in other locations at the same latitude; for instance, in Beijing, the ABL height is commonly below 2 km during the same seasons (He et al. 2006). Mihailovic et al. (2005) and Hasel et al. (2005) show that differences in ABL heights can be attributed to discrepancies in the environmental conditions at various places. Other studies conclude that surface conditions are strongly related to ABL heights. For instance, surface parameters such as albedo, soil moisture and near-surface wind conditions may play important roles in the development of the mixed layer. The development of the boundary layer is also strongly coupled to changes in the surface energy balance (Dolman et al. 1997). Thus, meteorological conditions that affect the surface energy balance also have an influence on the ABL height.

Despite our current knowledge of ABL heights, there has not yet been a study to characterize the extremely high ABL over north-west China. Therefore, our objective is to characterize a case over the Dunhuang area in north-west China and also to understand the surface and environmental parameters that influence the formation of the extremely deep ABL. An advanced research version of the weather research and forecasting (WRF) model (Skamarock et al. 2008) is employed to simulate these observed extreme boundary-layer heights in May 2000. The ability of the WRF model in simulating the ABL height over the arid areas is evaluated. Sensitivity experiments are also conducted to identify key parameters that contribute to the development of the extremely deep boundary layer.

The article is organized as follows: Sect. 2 describes the characteristics of the observed extremely deep convective boundary layer in late May 2000 over Dunhuang, which is in north-west China. The WRF model numerical simulation and sensitivity experiments are described in Sect. 3, results are discussed in Sect. 4, and concluding remarks are made in Sect. 5.

## 2 An Observed Extreme Atmospheric Boundary-Layer Height

Observations were obtained from Dunhuang (Fig. 1) during an intensive observational period from 25 May to 17 June 2000 in a field program (the so-called Duhuang Experiment, Zhang

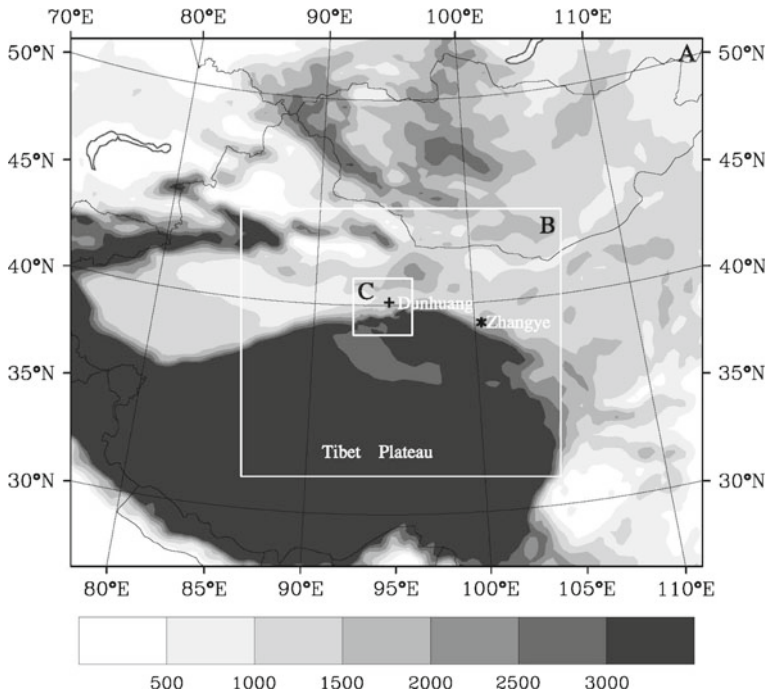


**Fig. 1** Map of terrain heights (*shaded contours*, unit: m) and model domains. The '+' sign denotes the centre of Dunhuang area and the '\*' sign denotes the centre of the Zhangye area

et al. 2001). The collected data include observations from surface micrometeorological stations and small-balloon soundings. Specifically, surface micrometeorological observations were obtained at the Shuang Dunzi Gobi station located at  $40.17^{\circ}\text{N}$ ,  $94.52^{\circ}\text{E}$  at an elevation of 1,150 m above sea level. The data include meteorological elements of wind speed and direction, air temperature, air humidity, soil temperature and components of surface radiation. The small-balloon sounding observation site was located at the Dunhuang Meteorological Bureau at  $40.15^{\circ}\text{N}$ ,  $94.68^{\circ}\text{E}$  at 1,140 m above sea level with a mean surface pressure of 873 hPa. The sounding data are available for the meteorological elements of wind speed and direction, air temperature and relative humidity from near surface to 6,000 m height, with a vertical resolution of 50 m for the height levels below 1,000 and 150 m above 1,000 m, respectively. The data were collected eight times daily at 0300, 0700, 1000, 1200, 1400, 1600, 1900 and 2300 Beijing Standard Time (BST), which are 1900, 2300, 0200, 0400, 0600, 0800, 1100 and 1500 UTC. We use UTC unless an additional explanation is given.

According to Heffter (1980) and Marsik et al. (1995), ABL height can be inferred from temperature measured from radiosondes and tether sondes. Specifically, by analyzing vertical profiles of potential temperature ( $\theta$ ), a possible elevated inversion, which is assumed to be a mark of the top of the mixed layer, can be identified. It defines the lowest inversion whose potential temperature lapse rate is equal to or larger than  $0.005 \text{ km}^{-1}$ , and the temperature difference between the inversion base and its top exceeds 2 K. The potential temperature profile shows a well-defined capping inversion under daytime convective conditions. The method is also used for the determination of the nighttime mixing height under a stable boundary

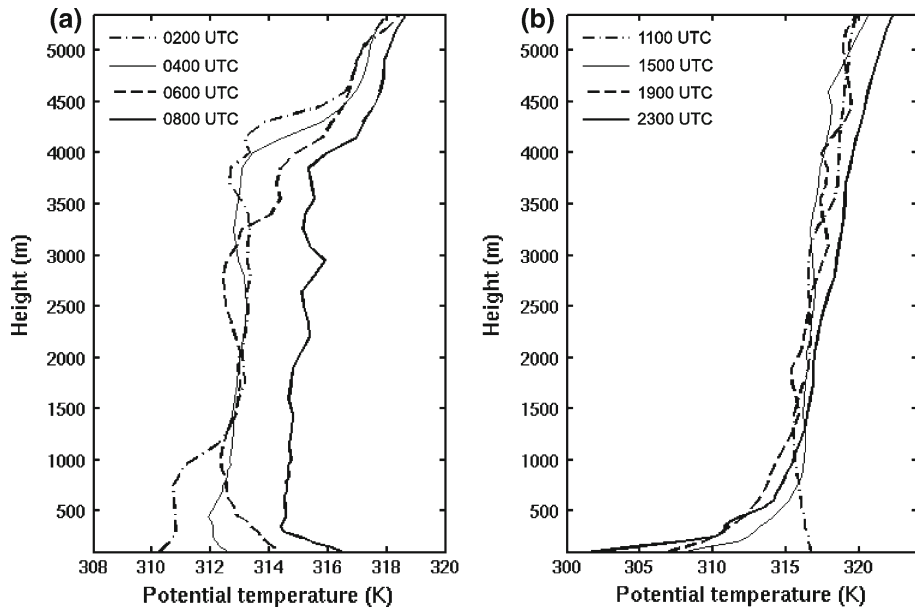


**Fig. 2** Potential temperature profiles over Dunhuang during **a** the daytime and **b** the nighttime on 29 May 2000

layer (Piringer et al. 1998). Based on these previous studies, the potential temperature with the same criteria is used for defining the ABL height over the Dunhuang area.

Figure 2 shows the profiles of atmospheric potential temperature on 29 May 2000 over the Dunhuang area. It is obvious that the profiles of the potential temperature are more vertically sloped during the daytime (Fig. 2a), compared with those during the nighttime (Fig. 2b). An obvious inflection point is located around 4-km height at 0400, 0600 and 0800 UTC, respectively, indicating the convective boundary-layer height during the daytime. The nocturnal lines of the potential temperature are oblique without reflection points but the gradients of potential temperature for three lines (1500, 1900, and 2300 UTC) are very small beneath about 700 m, which is the height of the stable boundary layer during the night. From the figure, the maximum ABL height during the daytime is seen to be as high as about 4 km on 29 May. For convenience, we define the *maximum ABL height* during any day as the *ABL height of the day*. Therefore, the ABL height of the day is 4 km on 29 May 2000.

As a typical case chosen for this study, a time series of ABL height is obtained for three consecutive days between 29 and 31 May, where it is found that the ABL heights during the day all exceed 2.5 km, with an overall average greater than 3.5 km. The greatest ABL heights during the day over these 6 days were over 4 km (29 May and 1 June). As illustrated in Fig. 3, the diurnal variation of ABL height reflects processes and changes within the boundary layer. Specifically, the inversion lip generated at nighttime ascends or is destroyed at sunrise, with mixing then active so that the new convective boundary layer quickly develops. After sunrise, the convective boundary-layer height increases and reaches its peak at noon (around 0800 UTC). Then, the next stable boundary layer is established during the night. This cycling process is associated with radiative warming and cooling that greatly influences the ABL height (Mok and Rudowicz 2004).

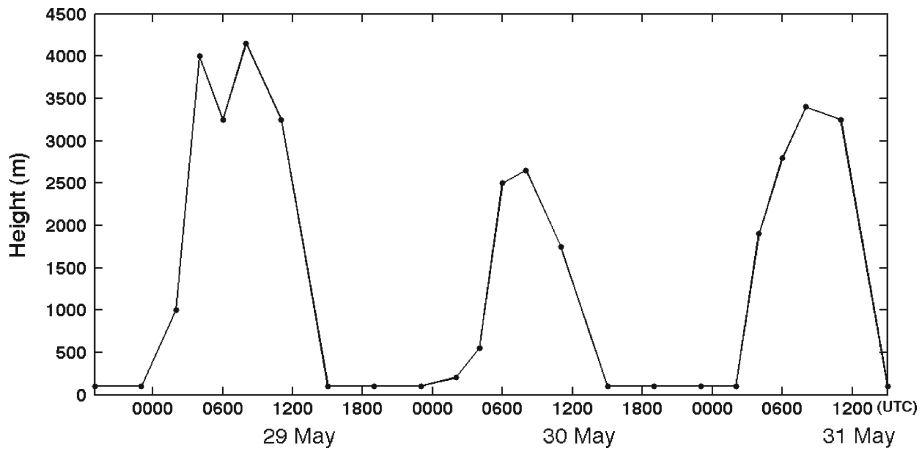


**Fig. 3** Time series of the observed diurnal variation of the ABL height during 29–31 May, 2000

The variation of ABL height during the day is also associated with surface and meteorological conditions. Comparing the evolution of observed solar radiation (figure not shown) with environmental winds over the 3 days, it is apparent that the wind speed on 29 May is stronger than the other 2 days as is the solar radiation. The wind profiles indicate well-mixed conditions with high wind speeds in the lower atmosphere during the daytime of 29 May (Fig. 4a). The wind shear is small and the boundary layer is extremely high. In contrast, the wind speed changes at about 2.5-km height on 30 May and at 3.0 km on 31 May. In addition, the relative humidity profiles (Fig. 4b) also reveal that the air mixes well in the atmosphere below about 3.5 km on 29 May.

Dolman et al. (1997) concluded that a greater boundary-layer depth can be observed in drier and warmer atmospheric conditions. Compared with Dunhuang, the ABL heights are much smaller at other stations nearby; specifically, Zhangye station (39.02°N, 100.42°E; Fig. 1) has a similar latitude to Dunhuang and is also located in an arid region in north-west China. Both stations are north of the Qilian Mountains. However, the common ABL heights during the daytime over Zhangye are about 2 km and are lower than those at Dunhuang during the same season. An early study by Zhang (2007) indicated that the difference in ABL heights between the two areas is attributed to the different evaporation and precipitation conditions. Dunhuang is an area that has plentiful sunshine and little precipitation. The annual precipitation is less than 40 mm and annual potential evaporation is commonly below 3,400 mm (Zhang et al. 2006), while Zhangye has more evaporation and precipitation. Ultimately, the main differences between Dunhuang and Zhangye are their surface conditions. Dunhuang is located in the Gobi area with very little vegetation coverage. In contrast, Zhangye is an area with abundant sunlight and fertile soil, making it an important agriculture area. In late spring, the landscape of Zhangye is covered by vegetation. Considering these factors, it is hypothesized that the surface conditions (such as albedo and soil moisture) over Dunhuang area are the main influencing factors for the extreme ABL height.

In order to examine the above hypothesis and the physical mechanisms that cause this extreme ABL height over the Dunhuang area, numerical simulations are conducted to simulate the extreme ABL heights during 29–31 May 2000.



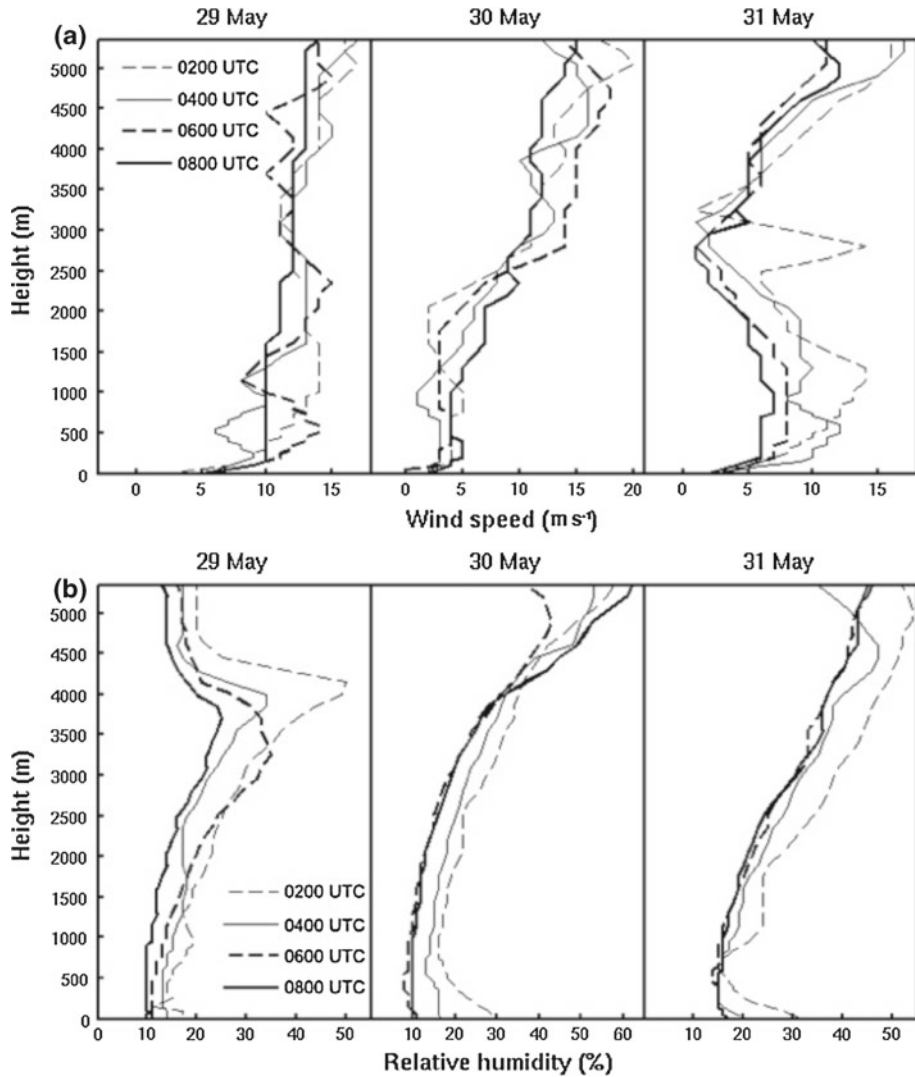


**Fig. 4** Vertical profiles of wind speed (a) and relative humidity (b) during the daytime on 29–31 May 2000 observed over Dunhuang

### 3 Numerical Simulations

#### 3.1 Numerical Model and Experimental Design

The numerical model used in this study is the mesoscale community WRF model. The WRF model was developed with multiple dynamic cores to supply both research and operational applications. One of the two dynamics solvers in the WRF software framework chosen in this study is an advanced research version of the WRF (ARW) solver, which is based on an Eulerian mass dynamical core with terrain-following vertical coordinates. The ARW solver was developed primarily at the National Center for Atmospheric Research, and features a



fully compressible, Eulerian non-hydrostatic core. The solver uses a second- or third-order Runge–Kutta time integration scheme with a small timestep for the acoustic and gravity-wave modes. Second- to sixth-order advection options are used in the horizontal and vertical spatial discretization. Arakawa C-grid staggering is applied in the horizontal grid. The WRF model has multiple physics options for microphysics, cumulus cloud, the surface, the planetary boundary layer and atmospheric radiation physics. More details are provided in [Skamarock et al. \(2008\)](#).

Considering the effect of terrain over the Tibetan Plateau (TP), a coarse domain (domain A in [Fig. 1](#)) is set with a centre at 40.17°N, 94.52°E and  $112 \times 94$  grid points at a horizontal resolution of 30 km. The domain includes the Tibetan Plateau. The second domain (domain B in [Fig. 1](#)) is nested inside of domain A with  $169 \times 142$  grid points at a resolution of 10 km. The third domain (domain C in [Fig. 1](#)) is set at  $94 \times 91$  grid points at a resolution of 3.3 km. A two-way interactive nested technique is used for achieving the high-resolution simulation. The vertical levels are divided into  $27\sigma$  layers from bottom to top with the model levels denser in the lower atmosphere from 900 to 600 hPa but relatively coarser above the 600-hPa level. The model physics option is set as follows: WRF single-moment six-class (WSM6) microphysical scheme ([Hong et al. 2004](#)), Rapid Radiative Transfer Model (RRTM, [Mlawer et al. 1997](#)) longwave radiation scheme, Dudhia shortwave radiation scheme ([Dudhia 1989](#)), a surface-layer Monin–Obukhov scheme, Yonsei University (YSU) planetary boundary-layer (PBL) scheme ([Hong and Pan 1996](#)), Kain–Fritsch cumulus scheme ([Kain and Fritsch 1993](#)) and the Noah land-surface model ([Chen and Dudhia 2001](#)).

In the YSU PBL scheme, the ABL height is defined by means of the bulk Richardson number in the process of integration ([Hong and Pan 1996](#); [Hong and Noh 2006](#)). The value of the ABL height corresponds to the critical bulk Richardson number and is obtained by linear interpolation between the two adjacent model levels. The critical bulk Richardson number is set at 0.5 and a revised non-local vertical diffusion scheme is applied in the model. The ABL top is defined with an explicit treatment of the entrainment layer. While the model has a more complex means of defining the ABL height, the ABL height defined by the WRF model was compared with those derived from the temperature profiles (as described in [Sect. 2](#)). The differences between the ABL heights obtained from two methods are less than 30 m.

With the initial time set at 1200 UTC 27 May 2000, the integration is forwarded 100 h to 1600 UTC 31 May 2000. The initial and boundary conditions are derived from the National Centers for Environmental Prediction/Department of Energy Reanalysis II (NCEP/DOE reanalysis II) data at a horizontal resolution of  $2.5 \times 2.5$  degrees.

### 3.2 Model Validation

The WRF model simulated time series of ABL heights is compared with observations ([Fig. 5a](#)). The simulated maximum heights of the 3 days (29, 30 and 31 May) are all above 2.5 km with an average of 3.5 km, agreeing well with the observations. The simulated maximum ABL height on 29 May is slightly lower than the observations, while the simulations on 30 and 31 May are slightly greater than the observations. Overall, the simulation has captured the major variations from the observations. The maximum differences in ABL heights between the simulated and observed values are less than 300 m.

In order to further evaluate the realism of the model simulation, the simulated ABL height for the day over Zhangye (as mentioned in the previous section) is compared with the simulation at Dunhuang ([Fig. 5b](#)). It is found that the ABL heights for the day in Zhangye are

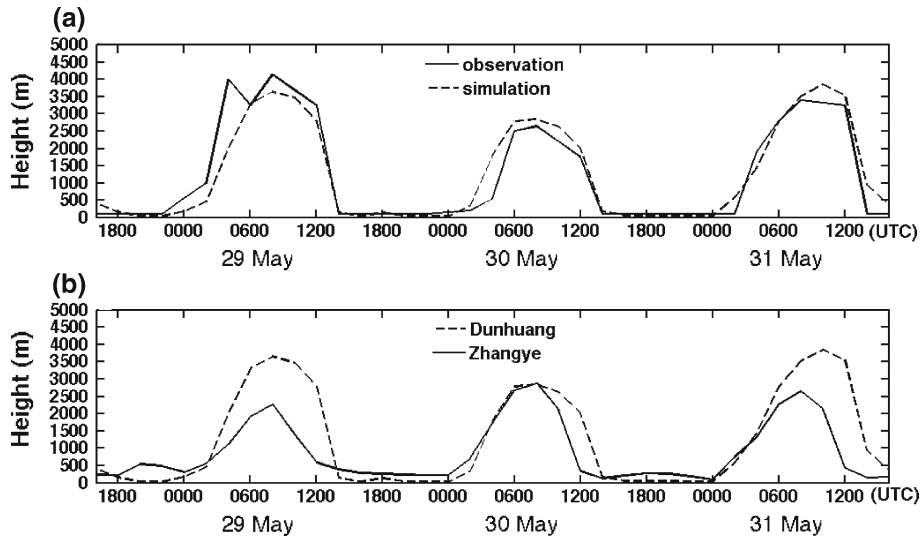


**Fig. 5** Time series of ABL heights during 29–31 May 2000. (a) Model simulation of ABL heights over Dunhuang, compared with the observations. (b) Model simulations of ABL height over Dunhuang compared with the simulated ABL height over Zhangye

between 2 and 3 km with an average of 2.6 km over 3 days, which is much less than the average of 3.5 km in Dunhuang. In accordance with the discussion of the two sites in the previous section, the model is able to distinguish the ABL heights over Dunhuang from Zhangye. This distinctiveness in simulated ABL heights between the two stations confirms that the WRF model simulation is reasonable.

### 3.3 Sensitivity Experiments

In order to examine the influence of surface and atmospheric conditions on the formation of the extremely deep boundary layer, two types of sensitive experiments are performed. One is done by changing model options, including the use of different forecast lead-times and land-surface schemes to investigate the impact of the specification of atmospheric conditions and near-surface conditions on the simulated ABL heights. The other is to evaluate the influence of perturbed surface parameters, including soil moisture and albedo to detect the influence of surface parameters on the simulated ABL height.

## 4 Results and Discussion

### 4.1 Sensitivity to the Forecast Lead Time

Changing the initial time means a change of forecast lead time and initial conditions or data input into the model. Figure 6 illustrates the model-simulated ABL height due to changing the initial time. With a shorter forecast lead-time, the simulated ABL height of the day generally decreases. Specifically, when initial time was set at 1200 UTC 26 May (3-day lead-time), the model generated the greatest ABL height out of all experiments because of the longest forecast lead-time. In contrast, if the initial time was set at 0000 UTC 29 May

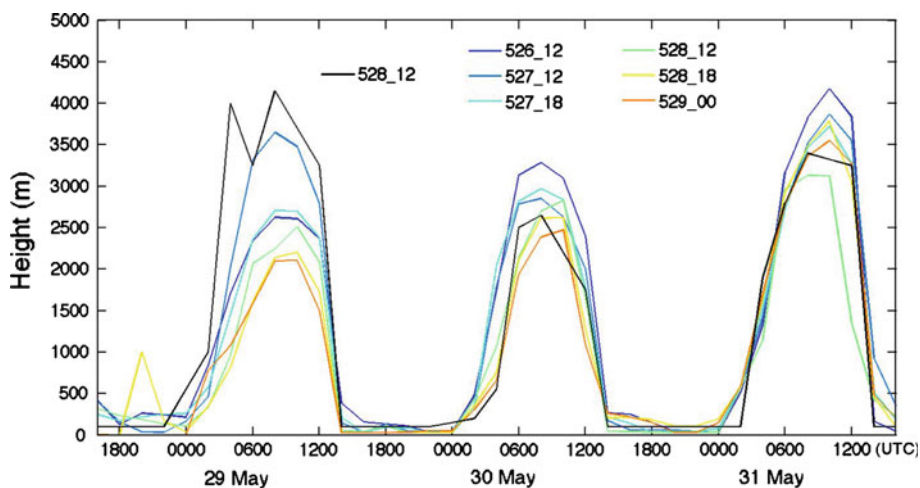


**Fig. 6** Diurnal variations of model simulated ABL height over Dunhuang during 29–31 May 2000 with different forecast lead-times, compared with observations ('obs'). '526\_12' means the initial time of the simulation is 1200 UTC 26 May. All other labels are similar

(zero lead-time), the simulation produced the lowest maximum boundary layer for all the 3 days. Meanwhile, the simulations are less accurate on 31 May than on 30 May. Of all the sensitivity experiments, the best simulation was generated when model integration started at 1200 UTC 27 May, as this captured the major observed variations of the ABL heights during the simulation period.

The different simulations of the ABL height for various initial times can be attributed to differences in the simulated meteorological conditions. Comparing the wind profiles valid at the same times during 29–31 May with simulations using different forecast lead-times (Figure omitted), it is obvious that the simulated wind profiles vary with different forecast lead-times. In reality, wind speed is a major factor that affects the formation of the extremely deep ABL. [Kossmann et al. \(1998\)](#) and [Kalthoff et al. \(1998\)](#) indicated that the large-scale airflow over the mountain range and thermally induced upslope winds have a strong influence on the development of the convective boundary-layer depth. Dunhuang is located in a valley between mountains to the south and north, where to the south is the great Tibetan Plateau (TP). Airflow is forced by the local terrain; the valley breeze (Fig. 7a) flows up the plateau during the daytime and the direction is changed in the morning as the mountain air flows down the plateau (Fig. 7b). The wind direction changes create updrafts and downdrafts that transfer momentum to the air over Dunhuang and enhance the mixing during the daytime, thus providing a dynamically advantageous environment in which to develop the extremely deep ABL.

The fact that various lead times result in different forecasts also implies that the initial conditions could be a key factor in determining the accurate simulation of the ABL heights of the day.

#### 4.2 Sensitivity to Land-Surface Schemes in WRF Model

With the same setting of the numerical simulation as mentioned in Sect. 3.1, two different land-surface models (LSMs) within the WRF model are applied in the numerical simu-

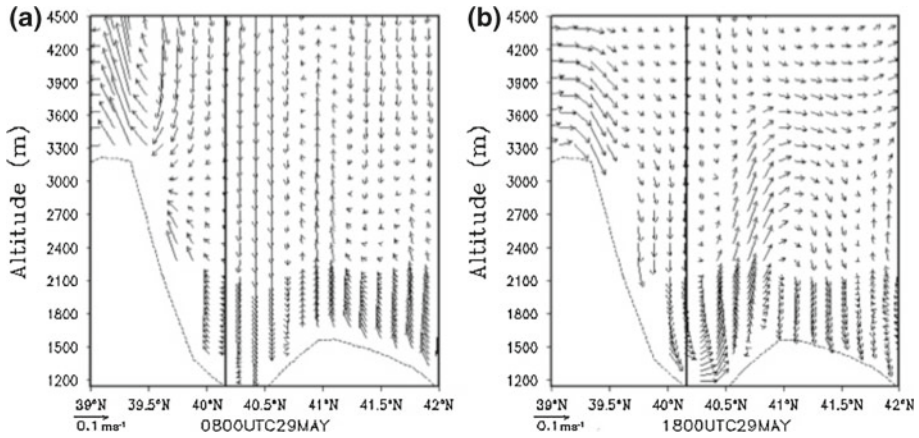


**Fig. 7** Longitudinal cross-section along 94.52°E for  $(v, w)$  wind vector, with the wind speed in the  $v$ -direction multiplied by 0.01 at (a) 1800 UTC 28 May (night-time) and (b) 0000 UTC 29 May (day-time). The short dash line is terrain height and the vertical solid line is located at 40.17°N, namely, over Dunhuang

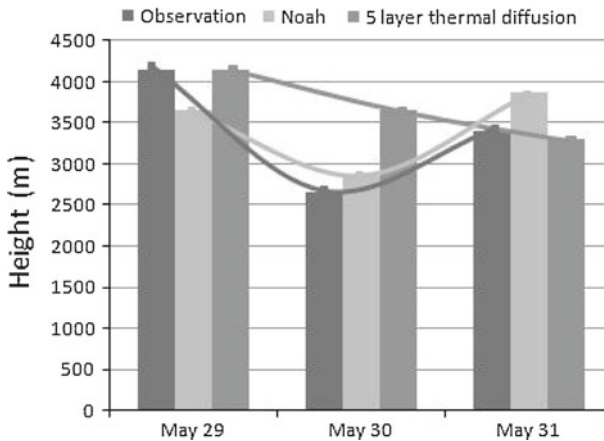


**Fig. 8** Model simulated maximum ABL height (ABL height of the day, in m) with different land-surface schemes (e.g. Noah LSM and five-layer thermal diffusion scheme) over Dunhuang on 29–31 May 2000, compared with observations

lations for the comparison: a five-layer thermal diffusion model and the Noah LSM. The five-layer thermal diffusion model is based on a five-layer soil temperature model for which the soil layers are defined at 0.01, 0.02, 0.04, 0.08, 0.16 m depths. Below these layers, the temperature is fixed at a deep-layer average. The Noah LSM is the successor to the Oregon State University (OSU) LSM, with the model developed jointly by NCAR, NCEP and the U.S. Air Force. It is a unified code for research and operational purposes, and sets the soil-layer thicknesses at 0.1, 0.3, 0.6 and 1.00 m from the top down. According to Skamarock et al. (2008), the model has the advantage of being consistent with the time-dependent soil fields provided in the analysis datasets.

Results from two sets of experiments are compared with the observations. A significant impact on the simulated ABL height of the day is found with the use of different LSMs (Fig. 8). The largest difference in the simulated ABL heights between the experiments with

**Table 1** Simulated ABL heights during the day over Dunhuang for 29–31 May for soil moisture perturbed at the initial time (1200 UTC 27 May), compared with a control simulation without soil moisture perturbation and observations (OBS)

Day	OBS (m)	-40% (m)	-20% (m)	-10% (m)	Control (m)	+10% (m)	+20% (m)	+40% (m)
29 May	4150	3915	3819	3754	3652	3589	3523	3336
30 May	2650	3029	2986	2941	2851	2836	2797	2724
31 May	3400	4146	4071	4052	3863	3714	3708	3468

“-40” means the soil moisture decreases 40% at the initial time. “+10” means the soil moisture increases 10% at the initial time. All other labels are similar

the Noah LSM and the five-layer thermal diffusion model reaches 802 m on 30 May. The maximum error in the ABL height produced by the five-layer thermal diffusion scheme is about 1,004 m. In addition, the variation of the ABL height simulated by the five-layer thermal diffusion scheme continuously decreases from 29 to 31 May. This is quite different behaviour from the observations, for which the variation shows a minimum with the lowest ABL height of the day occurring on 30 May. In contrast, the simulation with the Noah LSM scheme captured this variation during the 3 days, although the simulated ABL height of the day using the Noah LSM on 31 May is greater than that observed.

It should be noted that one of the main differences between the Noah LSM and the five-layer thermal diffusion scheme is that the Noah LSM requires the input of the soil moisture. The soil moisture in a five-layer thermal diffusion scheme, however, is a seasonal-dependent constant value. Considering this factor, the sensitivity of the WRF simulated ABL height to the soil moisture parameters is addressed below.

#### 4.3 Sensitivity to Soil Moisture

Soil moisture is an important factor that affects the ABL height (Desai et al. 2006), directly influencing the distribution at the surface of solar radiation energy that is converted into sensible and latent heat. In order to investigate the sensitivity of the simulation results to the soil moisture, numerical simulations were conducted with perturbed soil moisture conditions. Table 1 shows the impact of the perturbed initial soil moisture (at 1200 UTC 27 May) on the simulated ABL heights. Specifically, when soil moisture values were decreased, the simulation of ABL height during the day notably increased over the following 3 days. In contrast, the ABL height evidently decreased with the increase of the initial soil moisture. For instance, in the numerical experiments, if the value of the initial soil moisture decreased by 40% of its original value, then the ABL height during the day increased by 263, 177 and 284 m on 29, 30 and 31 May, respectively. If the value of the initial soil moisture increased by 40% of its original value, then the ABL height of the day decreased by 316, 127 and 394 m on 29, 30 and 31 May, respectively. It should be noted that even if the soil moisture increased by 40% (about  $0.06\text{--}0.09\text{ kg m}^{-3}$ ) at the initial time, its magnitude only reached the average level for the Zhangye area, which is also a dry, arid region in north-west China.

#### 4.4 Sensitivity to Surface Albedo

The radiation effect is one of the key factors that determines the ABL height. Among other factors, surface albedo has a direct impact on the reflected incoming solar radiation, and so

**Table 2** Simulated ABL height during the day over Dunhuang during 29–31 May using monthly albedo value (“USE”) and perturbing albedo (“–25” and “+25”), compared with control simulation using land use (“Control”)

Day	OBS (m)	Control (m)	USE (m)	+25% (m)	–25% (m)
May 29	4150	3652	3983	3826	4092
May 30	2650	2851	2943	2764	3123
May 31	3400	3863	4114	3897	4233

The label ‘–25’ and ‘+25’ mean that the albedo value decreases and increases 25% in the experiments, respectively

is closely related to the upward sensible heat flux. Therefore, sensitivity experiments were conducted with a perturbed surface albedo.

The input to the WRF model pre-process contains two-dimensional static terrestrial fields of albedo, terrain elevation and vegetation/land-use type. Following the common procedure in the WRF model pre-process, in the control simulation described above, the land-use value of the albedo is used. In one of the sensitivity experiments, the monthly albedo values (which are different from the land-use values) are used. Table 2 indicates that the simulated ABL heights during the day in all 3 days increased with the use of the monthly albedo values. The maximum increase in the simulated ABL height of the day on 29 May reached as high as 331 m, which is more than 9% of the simulated height in the control experiment. The errors in the ABL heights on 30 and 31 May also became larger; the error on 31 May reached 715 m, which is 21% of the observed maximum ABL height. Overall, numerical simulations of the ABL height are sensitive to the use of the surface albedo value.

Additional experiments were also performed by perturbing albedo to  $\pm 25\%$  of the land-use value. Table 2 shows that the simulated ABL heights of the day are further increased by 150–200 m when albedo value is reduced by 25%. In contrast, the ABL heights decreased by 100–170 m when the albedo is increased by 25%.

## 5 Concluding Remarks

An extremely high atmospheric boundary layer was observed in late spring at Dunhuang, an arid area in north-west China, with the average of the observed ABL heights over 3 days being above 3.5 km. The maximum ABL height during the daytime exceeded 4 km on 29 May 2000. Since the depth of ABL is commonly about 1–2 km in many locations at the same latitude, these observed ABL heights over Dunhuang are extremely high.

A numerical simulation was performed to evaluate the capability of the WRF numerical model in simulating these extreme ABL heights. Results demonstrate that the model is capable of capturing the major characteristics of observed extreme ABL heights. However, the choices of land-surface physical options in the WRF model and forecast lead-times affect the simulation results. Sensitivity studies also show that the initial soil moisture is an influencing factor in producing this extremely high ABL. When the value of soil moisture increased by about 40% of its original value, the simulated ABL height decreased by more than 10%. In contrast, decreases of the initial soil moisture resulted in increases in the ABL height. In addition, surface albedo also has a significant influence on the ABL height. The sensitivity of the simulated ABL heights to changes in soil moisture and albedo explains, at least partly, the reasons for the extremely high ABL over the area of interest. To some extent, surface



conditions such as soil moisture and albedo combined with atmospheric conditions (such as wind-speed conditions) are the determining factors for the formation of an extremely deep ABL over the Dunhuang area. Since Dunhuang is one of the most arid regions in China, its low soil moisture and significant flows forced by local terrain offer favourable conditions in generating the extreme boundary-layer height.

**Acknowledgements** This study is supported by the U.S. National Science Foundation Award No. ATM-0833985, the Chinese Science and Technology Base Funding No. 2008BAC40B04 and No. 2009BAC53B02 and the National Natural Science Foundation of China Grant No. 40830597. The first author (MM) is also supported by the Chinese overseas scholarship sponsored by the State Department of Education of China. Computer time utilization permission granted by the Centre for High Performing Computer (CHPC) at the University of Utah is gratefully acknowledged.

## References

- Chen F, Dudhia J (2001) Coupling an advanced land-surface/hydrology model with the Penn State/NCAR MM5 modeling system. Part I: Model description and implementation. *Mon Weather Rev* 129:569–585
- Culf AD (1993) The potential for estimating regional sensible heat flux from convective boundary layer growth. *J Hydrol* 146:235–244
- Culf AD, Fisch G, Malhi Y, Nobre CA (1997) The influence of the atmospheric boundary layer on carbon dioxide concentrations over a tropical forest. *Agric For Meteorol* 85:149–158
- Davies F, Middleton DR, Bozier KE (2007) Urban air pollution modelling and measurements of boundary layer height. *Atmos Environ* 41:4040–4049
- Desai AR, Davis KJ, Senff CJ, Ismail S, Browell EV, Stauffer DR, Reen BP (2006) A case study on the effects of heterogeneous soil moisture on mesoscale boundary-layer structure in the southern great plains, USA Part I: Simple prognostic model. *Boundary-Layer Meteorol* 119:195–238
- Dolman AJ, Culf AD, Bessemoulin P (1997) Observations of boundary layer development during the HAPEX-Sahel intensive observation period. *J Hydrol* 188:998–1016
- Dudhia J (1989) Numerical study of convection observed during the winter monsoon experiment using a mesoscale two-dimensional model. *J Atmos Sci* 46:3077–3107
- Garratt JR (1992) *The atmospheric boundary layer*. Cambridge University press, UK, 316 pp
- Garratt JR, Pearman GI (1973) CO<sub>2</sub> concentration in the atmospheric boundary layer over South-East Australia. *Atmos Environ* 7:1257–1266
- Gryning SE, Holtslag AAM, Irwin JS, Sivertsen B (1987) Applied dispersion modeling based on meteorological scaling parameters. *Atmos Environ* 21:79–89
- Hasel M, Kottmeier Ch, Corsmeier U, Wieser A (2005) Airborne measurements of turbulent trace gas fluxes, analysis of eddy structure in the convective boundary layer over complex terrain. *Atmos Res* 74:381–402
- He QS, Mao JT, Chen JY, Hu YY (2006) Observational and modeling studies of urban atmospheric boundary-layer height and its evolution mechanisms. *Atmos Environ* 40:1064–1077
- Heffter JL (1980) Transport layer depth calculations. In: *Proceedings of the 2nd joint conference on applications of air pollution modelling*. American Meteorological Society, pp 787–791
- Hong SY, Noh Y (2006) A new vertical diffusion package with an explicit treatment of environment processes. *Mon Weather Rev* 134:2318–2341
- Hong SY, Pan HL (1996) Nonlocal boundary layer vertical diffusion in a medium-range forecast model. *Mon Weather Rev* 124:2322–2339
- Hong SY, Dudhia J, Chen S-H (2004) A revised approach to ice microphysical processes for the bulk parameterization of clouds and precipitation. *Mon Weather Rev* 132:103–120
- Kain JS, Fritsch JM (1993) The role of the convective “trigger function” in numerical prediction of mesoscale convective systems. *Meteorol Atmos Phys* 49:93–106
- Kalthoff N, Binder HJ, Kossmann M, Vöglin R, Corsmeier U, Beyrich F, Schlager H (1998) Temporal evolution and spatial variation of the boundary layer over complex terrain. *Atmos Environ* 32:1179–1194
- Kossmann M, Vöglin R, Corsmeier U, Vogel B, Fiedler F, Binder HJ, Kalthoff N, Beyrich F (1998) Aspects of the convective boundary layer structure over complex terrain. *Atmos Environ* 32:1323–1348
- Kumar M, Mallik C, Kumar A, Mahanti NC, Shekh AM (2010) Evaluation of the boundary layer depth in semi-arid region of India. *Dyn Atmos Oceans* 49:96–107
- Marsik FJ, Fischer KW, McDonald TD, Samson PJ (1995) Comparison of methods for estimating mixing height used during the 1992 Atlanta field intensive. *J Appl Meteorol* 34:1802–1814



- Mihailovic DT, Rao ST, Alapaty K, Ku JY, Arsenic I, Lalic B (2005) A study on the effects of subgrid-scale representation of land use on the boundary layer evolution using a 1-D model. *Environ Model Softw* 20:705–714
- Mlawer EJ, Taubman SJ, Brown KD, Iacono MJ, Clough SA (1997) Radiative transfer for inhomogeneous atmosphere: RRTM, a validated correlated-k model for the long-wave. *J Geophys Res* 102:16663–16682
- Mok TM, Rudowicz CZ (2004) A lidar study of the atmospheric entrainment zone and mixed layer over Hong Kong. *Atmos Res* 69:147–163
- O'Brien JJ (1970) A note on the vertical structure of eddy exchange coefficient in the planetary boundary layer. *J Atmos Sci* 27:1213–1215
- Oncley SP, Buhr M, Lenxchow DH, Davis D, Semmer SR (2004) Observations of summertime NO fluxes and boundary-layer height at the South Pole during ISCAT 2000 using scalar similarity. *Atmos Environ* 38:5389–5398
- Piringer M, Baumann K, Langer M (1998) Summertime mixing heights at Vienna, Austria, estimated from vertical soundings and by a numerical model. *Boundary-Layer Meteorol* 89:24–45
- Raman S, Templeman B, Templeman S, Holt T, Murthy AB, Singh MP, Agarwal P, Nigam S, Prabhu S, Ameenullah S (1990) Structure of the Indian southwesterly pre-monsoon and monsoon boundary layers: observations and numerical simulation. *Atmos Environ* 24A:723–734
- Seibert P, Beyrich F, Gryning SE, Joffre S, Rasmussen A, Tercier P (2000) Review and intercomparison of operational methods for the determination of the mixing height. *Atmos Environ* 34:1001–1027
- Skamarock WC, Klemp JB, Dudhia J, Gill DO, Barker DM, Duda MG, Huang X, Wang W, Powers JG (2008) A description of the advanced research WRF version 3. NCAR Technical note NCAR/TN-475+STR, 113 pp
- Zhang Q (2007) Study on depth of atmospheric thermal boundary layer in extreme arid desert regions. *J Desert Res* 27:614–620
- Zhang Q, Wei G, Huang R (2001) The bulk transfer coefficients of the atmospheric momentum and sensible heat over desert and Gobi in arid climate region of Northwest China. *Sci China Ser D* 31:783–792
- Zhang Q, Wang S, Li Y (2006) Study on physical mechanism of influence on atmospheric boundary layer depth in the arid regions of Northwest China. *Acta Meteorol Sin* 20:1–12